QUARTERLY OF APPLIED MATHEMATICS
APRIL 1980

WAVE PROPAGATION IN AN ELASTIC HALF-SPACE DUE TO SURFACE PRESSURE OVER A NON-UNIFORMLY CHANGING CIRCULAR ZONE*

BY

L. M. BROCK

University of Kentucky

Abstract. Two problems of pressure distributions applied to an elastic half-space over a circular pressure zone whose center is fixed but whose radius changes non-uniformly with time are considered. In one case, the pressure depends only on time; in the other case, the pressure varies with the radial distance from the pressure zone center. Complete transform solutions are obtained and several wave propagation aspects are briefly studied, with emphasis on the Rayleigh pole contributions and the associated propagating singularities. The effects of some specific zone time-histories on the Rayleigh pole disturbances at the half-space surface are considered. Some characteristics of a given time-history appear to be manifested in the corresponding disturbance.

1. Introduction. The dynamic analysis of elastic solids whose surfaces are subjected to pressures over certain regions has applications in seismology and structural dynamics. Lamb [1], Pekeris [2] and Chao, Bleich and Sackman [3] have treated the special case of the fixed normal point load on a half-space. Problems of surface pressures applied over axisymmetric areas which expand at constant rates have been considered by Craggs [4], Atkinson [5] and Gakenheimer [6]. The work of [4] and [5] examined a uniform pressure while [6] treated a class of pressure loads which give a constant force on the half-space. All three analyses were exact. Miles [7], Baron and Check [8], Ablow [9], Blowers [10] and Tong [11] have studied variable expansion rates. However, the solutions in [7, 8] and [9] are valid only at points near, respectively, the half-space surface and the wavefronts. The work of [10] and [11] considered the special cases of surface pressures whose application areas expand at a rate inversely proportional to the square-root of time. More recently, Freund [12, 13] gave exact solutions for the plane-strain problems of time-independent line and semi-infinite pressure loadings extending at largely arbitrary non-uniform rates on a half-plane.

The present work considers two related three-dimensional problems of pressure distributions applied without friction over a time-varying zone on the surface of a linearly elastic, isotropic, homogeneous elastic half-space. The zone is a circle with its center fixed on the half-space and a radius which changes non-uniformly with time. In one problem, the pressure distribution is spatially invariant but time-dependent, while in the other problem, the distribution is time-independent but varies with the radial distance from the

* Received November 30, 1978; revised version received June 11, 1979.

pressure zone center. In the former case, the half-space is initially undisturbed. In the latter case, however, the pressure distribution may initially be quasi-statically applied over a fixed zone. The time rate of change of the zone radius and the time and spatial variations in the respective pressure distributions are largely arbitrary. In the next three sections, the solutions for the time-dependent pressure distribution are presented in some detail. In Sec. 5 the spatially-varying pressure distribution solution is given largely by analogy. Subsequently, some wave propagation aspects of the problems are discussed, with particular attention focusing on the Rayleigh pole contributions.

2. The time-dependent pressure distribution. The problem geometry is shown in Fig. 1a where $z \geq 0$ defines the half-space and r, θ, z are cylindrical coordinates. For convenience the variable $s = c_1 x$ (time) is introduced, where c_1, c_2 and μ are, respectively, the dilatational and rotational wave speeds and the shear modulus in the half-space. Prior to $s = 0$ the half-space is at rest. For $s \geq 0$ the pressure distribution $f(s)$ is applied without friction over the zone $r \leq h(s)$. The functions h and f are at least piecewise smooth and finite for finite $s \geq 0$. Here $h \geq 0$, $s \geq 0$ and both f and h may take on negative values, where $(\cdot) \equiv d(\ )/ds$, but $\dot{h} < 0$ only when $h > 0$.

Because of axial symmetry, the tangential displacement and all θ-dependence vanish. The boundary conditions on the half-space surface $z = 0$, $r > 0$ are then

$$\sigma_z = -f(s)H[h(s) - r], \qquad \sigma_{rz} = 0 \tag{1a,b}$$

when $s > 0$, while for r, $z > 0$ the initial conditions are

$$s \leq 0\text{: } u, w \equiv 0. \tag{2}$$

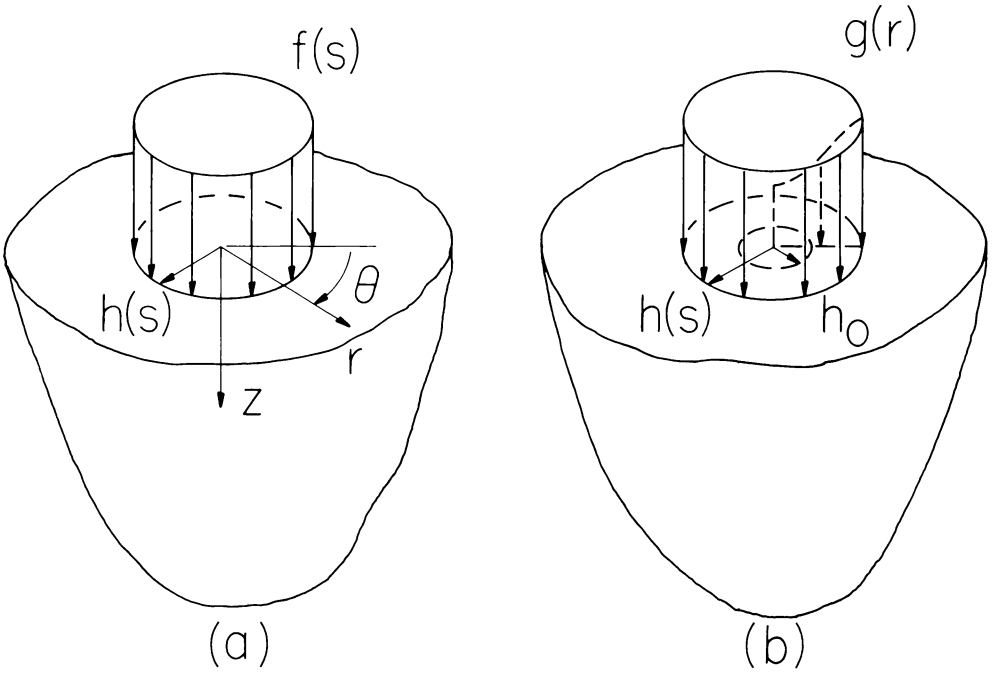

FIG. 1. (a) Time-dependent pressure distribution, (b) spatially-varying pressure distribution.

Here u and w are the radial (r) and axial (z) displacements while $H(\ )$ is the Heaviside step function. The governing equations for $r, z, s > 0$ are

$$\Delta_{,r} + 2m^2\omega_{,z} = \ddot{u}, \qquad \Delta_{,z} - 2m^2 r^{-1}(r\omega)_{,r} = \ddot{w} \tag{3a,b}$$

where Δ and ω are the dilatation and rotation defined by

$$\Delta = w_{,z} + r^{-1}(ru)_{,r}, \qquad 2\omega = u_{,z} - w_{,r}. \tag{4}$$

Here $(\ )_{,a} \equiv \partial(\ )/\partial a$ while $m = c_2/c_1$ $(0 < m < 1/\sqrt{2})$. The pertinent constitutive equations are

$$\frac{m^2}{\mu}\sigma_z = w_{,z} + (1 - 2m^2)r^{-1}(ru)_{,r}, \qquad \frac{1}{\mu}\sigma_{rz} = w_{,r} + u_{,z}. \tag{5}$$

Also, u and w are bounded above almost everywhere in $r, z > 0$ for finite s.

3. Transform solution. The Laplace transform and Hankel transform of order v [14]

$$L(F) = \hat{F} = \int_0^\infty F(s)e^{-ps}\,ds, \qquad H_v(F) = F^v = \int_0^\infty rF(r)J_v(\xi r)\,dr \tag{6a,b}$$

over $s > 0$ and $r > 0$ are employed, where p is real and positive and large enough to insure convergence of (6a) while ξ is in general complex. Here J_v is the Bessel function of order v. Operating on (3a,b) with (6) for $v = 1$ and $v = 0$, respectively, in view of (2) and (4) and requiring that u, w for $z > 0$ behave no worse than $O(r^{-\delta})$, $\delta < 1$ as $r \to 0$ yields

$$m^2\hat{u}^1_{,zz} - \alpha^2\hat{u}^1 + \xi(m^2 - 1)\hat{w}^0_{,z} = 0, \qquad \alpha = \sqrt{(p^2 + \xi^2)} \tag{7}$$

$$\hat{w}^0_{,zz} - m^2\beta^2\hat{w}^0 + \xi(1 - m^2)\hat{u}^1_{,z} = 0, \qquad \beta = \sqrt{(p^2/m^2 + \xi^2)} \tag{8}$$

for $z > 0$. For p real and positive α, β are defined in the complex ξ-plane cut along $\mathrm{Re}(\xi) = 0$, $|\mathrm{Im}(\xi)| > p$ and $|\mathrm{Im}(\xi)| > p/m$, respectively, so that $\mathrm{Re}(\alpha)$, $\mathrm{Re}(\beta) \geq 0$. Similarly, from (1) and (5) it can be shown that

$$\hat{\sigma}^0_z = \frac{-1}{\xi}\int_0^\infty f(t)h(t)J_1[\xi h(t)]e^{-pt}\,dt, \qquad \hat{\sigma}^1_{rz} = 0 \tag{9}$$

$$\frac{m^2}{\mu}\hat{\sigma}^0_z = \hat{w}^0_{,z} + (1 - 2m^2)\xi\hat{u}^1, \qquad \frac{1}{\mu}\hat{\sigma}^1_{rz} = \hat{u}^1_{,z} - \xi\hat{w}^0 \tag{10}$$

for $z = 0$ and $z > 0$, respectively. Solutions to (7)–(10) which are bounded as $z \to \infty$ are

$$\hat{u}^1 = Ae^{-\alpha z} + Be^{-\beta z}, \qquad \hat{w}^0 = \frac{\alpha}{\xi}Ae^{-\alpha z} + \frac{\xi}{\beta}Be^{-\beta z} \tag{11a,b}$$

$$\mu R(A, B) = (-\beta^2 - \xi^2, 2\alpha\beta)\int_0^\infty fhJ_1(\xi h)e^{-pt}\,dt, \qquad R = 4\xi^2\alpha\beta - (\beta^2 + \xi^2)^2 \tag{12a,b}$$

where R is a form of the Rayleigh function with simple zeros at $\xi = \pm ip/m_R$, $m_R = c_R/c_1$. Here $c_R (0 < c_R < c_2)$ is the Rayleigh wave speed. In (12) and similar integrals in the sequel, the t-dependence of f and h is understood.

4. Transform inversions. The inverse Hankel transform of order v is defined [14] as

$$F(r) = \int_{i\xi_0}^{i\xi_0 + \infty} \xi J_v(\xi r) F^v \, d\xi \tag{13}$$

where the real constant ξ_0 is chosen so that the integration path lies in the region of analyticity for F^v and convergence of (6b). Eqs. (11)–(13) show that we can choose $\xi_0 = 0$. Then substitution of (11a) into (13) yields the Laplace transform

$$\mu\hat{u} = \int_0^\infty f h e^{-pt} \int_0^\infty \xi J_1(\xi r) J_1(\xi h)[2\alpha\beta e^{-\beta z} - (\beta^2 + \xi^2)e^{-\alpha z}] \frac{d\xi}{R} \, dt. \tag{14}$$

To obtain the inverse transform of (14), the Cagniard-de Hoop [15] scheme is used. Therefore, because p is real and positive, the transformations

$$\xi = pq, \qquad \alpha = pa, \qquad \beta = pb, \qquad R = p^4 D \tag{15}$$

$$a = \sqrt{(1 + q^2)}, \qquad b = \sqrt{(m^{-2} + q^2)}, \qquad D = 4q^2 ab - (b^2 + q^2)^2 \tag{16}$$

are introduced, where clearly the behavior of a, b, D in the complex q-plane follows from that for α, β, R in the ξ-plane by setting $p = 1$. These transformations, the well-known relations [16]

$$J_1(x) = -\frac{dJ_0(x)}{dx}, \qquad J_0(x) = \frac{2}{\pi}\int_0^1 \frac{\cos vx}{\sqrt{(1 - v^2)}} \, dv \tag{17}$$

and some simple manipulations are used to rewrite the first term in (14) as

$$\frac{2}{\pi^2 r}\int_0^\infty f e^{-pt} \int_0^h \frac{x}{X}\int_0^r \frac{y}{Y}\int_0^\infty 2ab\frac{q}{D} e^{-pbz}[\cos pq(x - y) - \cos pq(x + y)] \, dq \, dy \, dx \, dt, \tag{18}$$

$$X = \sqrt{(h^2 - x^2)}, \qquad Y = \sqrt{(r^2 - y^2)}. \tag{19}$$

Recognition that the integrands are real for real q allows the q-integration to be written as

$$\mathrm{Re}\int_0^\infty 2ab\frac{q}{D} e^{-pbz}(e^{ipq|x-y|} - e^{ipq(x+y)}) \, dq. \tag{20}$$

The Cauchy theorem is used to switch the original q-integration path to Cagniard contours in the q-plane along which the exponentials in (20) assume the form e^{-pn} where n is real and positive. Thus, it is readily shown that (20) becomes

$$\mathrm{Re}\int_{z/m}^\infty U_b[q_b^+(n)]e^{-pn} \, dn - \mathrm{Re}\int_{z/m}^\infty U_b[q_b^-(n)]e^{-pn} \, dn, \; U_b(q) = 2ab\frac{q}{D}\frac{dq}{dn} \tag{21}$$

where for $z \le mn \le \rho_\pm$ and $mn \ge \rho_\pm$, respectively,

$$q_b^\pm(n) = iv_b^\pm(n), \qquad \rho_\pm^2 v_b^\pm(n) = nr_\pm - z\sqrt{(m^{-2}\rho_\pm^2 - n^2)}, \tag{22}$$

$$\rho_\pm^2 q_b^\pm(n) = inr_\pm + z\sqrt{(n^2 - m^{-2}\rho_\pm^2)}, \tag{23}$$

$$\rho_\pm = \sqrt{(z^2 + r_\pm^2)}, \qquad r_+ = x + y, \qquad r_- = |x - y|. \tag{24}$$

Eq. (23) indicates that the Cagniard contours include hyperbolae in the first quadrant of the q-plane with vertices $q_b^\pm = ir_\pm/m\rho_\pm$ and asymptotes $\arg(q_b^\pm) = \tan^{-1}(r_\pm/z)$. As the

hyperbolae are traversed from left to right, n varies from $m^{-1}\rho_{\pm}$ to ∞. Eq. (22) shows that the remaining portions of the Cagniard contours follow the Im(q)-axis from $q = 0$ to the corresponding hyperbola vertex. As the contours are traversed from $q = 0$ to $q = ir_{\pm}/m\rho_{\pm}$, n varies from z/m to $m^{-1}\rho_{\pm}$. It is understood that $\mathrm{Re}(q) = 0^{+}$.

In view of (21), the exponentials in (18) are the Laplace transforms of the Dirac delta function $\delta(s - t - n)$ [14]. The sifting property of the delta function can be used to eliminate the n-integration. Similar results hold for the second term in (14), so that for r, z, $s > 0$

$$\mu\pi^2 ru = 2\int_0^s f \int_0^h \frac{x}{X}\int_0^r \frac{y}{Y}\,\mathrm{Re}\; U(s-t)\,dy\,dx\,dt, \tag{25}$$

$$U(n) = \{U_a[q_a^+(n)] - U_a[q_a^-(n)]\}H(n - z) + \{U_b[q_b^-(n)] - U_b[q_b^+(n)]\}H(n - z/m), \tag{26}$$

$$U_a(q) = (b^2 + q^2)\frac{q}{D}\frac{dq}{dn}, \tag{27}$$

where $q_a^{\pm}$ follows from (22)–(24) by setting $m = 1$. A completely analogous procedure can be followed for the inversion of (11b) with the result that for r, z, $s > 0$

$$\mu\pi^2 w = 2\int_0^s f \int_0^h \frac{x}{X}\int_0^r \frac{1}{Y}\,\mathrm{Im}\; W(s-t)\,dy\,dx\,dt, \tag{28}$$

$$W(n) = \{W_b[q_b^+(n)] + SW_b[(q_b^-(n)]\}H(n - z/m) - \{W_a[q_a^+(n)] + SW_a[q_a^-(n)]\}H(n - z), \tag{29}$$

$$W_a(q) = (b^2 + q^2)\frac{a}{D}\frac{dq}{dn}, \qquad W_b(q) = 2q^2\frac{a}{D}\frac{dq}{dn}, \qquad S = \mathrm{sgn}(x - y). \tag{30}$$

It should be noted in light of (22)–(24) that the characteristic transformations

$$\sqrt{2}x = k - l, \qquad \sqrt{2}y = k + l, \qquad dx\,dy = dk\,dl \tag{31}$$

(see Fig. 2) into (25) and (28) allows a partial uncoupling of the $q^{\pm}$-terms in evaluating the multiple integrals. This may prove convenient in certain instances. However, as Fig. 2 indicates, determining the k and l integration limits for given values of r and h can be complicated.

5. The spatially-varying pressure distribution. The problem geometry for the spatially-varying pressure distribution is shown in Fig. 1b, where $r \leq h_0$ defines the initial pressure zone. Prior to $s = 0$ the half-space is in quasi-static equilibrium under the pressure distribution $g(r)$ applied without friction over the initial zone. For $s \geq 0$ the pressure zone is defined by $r \leq h(s)$. The function g is at least piecewise smooth and finite for finite $r \geq 0$. As in Secs. 2–4, the function $h \geq 0$, $s \geq 0$ is at least piecewise smooth and finite for finite $s \geq 0$. Both g and $\dot{h}$ may take on negative values, but $\dot{h} < 0$ only when $h > 0$.

Because the wave propagation problem is of chief interest, the superposition-related problem obtained by subtracting the initial quasi-static results from the complete solution is considered. Again, axial symmetry requires that the tangential displacement and θ-dependence vanish. Then, the boundary conditions on the half-space surface $z = 0$, $r > 0$ are

$$\sigma_z = g(r)H(h_0 - r) - g(r)H[h(s) - r], \qquad \sigma_{rz} = 0 \tag{32}$$

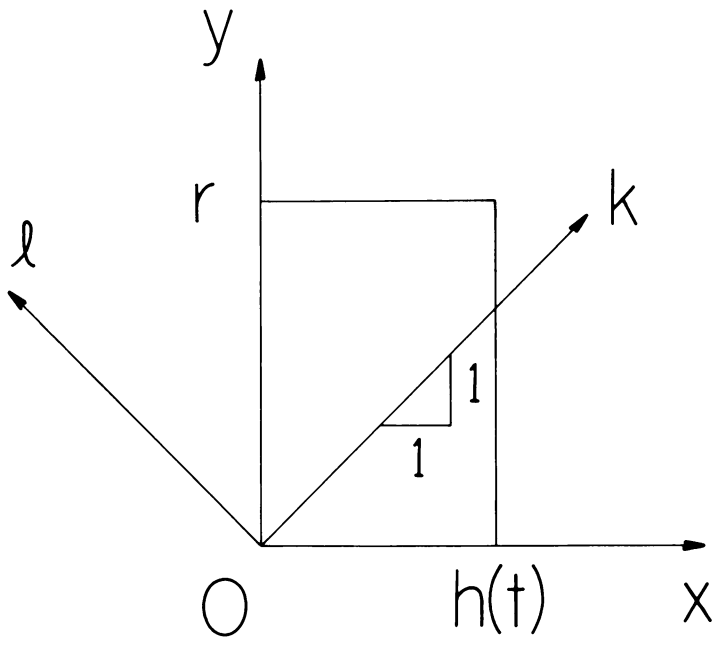

FIG. 2. Characteristic integration variable transformations.

when $s > 0$. The remaining conditions and governing equations for this problem are identical to those given by (2)–(5). The transform techniques in Sec. 3 can be applied to (32) and (2)–(5) with the result that (7), (8) and (10) are again valid, but (9) is replaced by

$$\hat{\sigma}_z^0 = \frac{-1}{p}\int_0^\infty g(h)h\dot{h}J_0(\xi h)e^{-pt}\,dt, \qquad \hat{\sigma}_{rz}^1 = 0 \tag{33}$$

Eqs. (7), (8), (10) and (33) yield the solutions (11) but (12a) is replaced by

$$\mu pR(A, B) = (-\beta^2 - \xi^2, 2\alpha\beta)\xi \int_0^\infty g(h)h\dot{h}J_0(\xi h)e^{-pt}\,dt. \tag{34}$$

Inversion of the transforms (11) in view of (34) follows the same pattern outlined in Sec. 4. The results are that for $r, z, s > 0$

$$\mu\pi^2 ru = 2\int_0^s g(h)h\dot{h}\int_0^h \frac{1}{X}\int_0^r \frac{y}{Y}\,\mathrm{Im}\;U(s-t)\,dy\,dx\,dt, \tag{35}$$

$$\mu\pi^2 w = 2\int_0^s g(h)h\dot{h}\int_0^h \frac{1}{X}\int_0^r \frac{1}{Y}\,\mathrm{Re}\;W(s-t)\,dy\,dx\,dt, \tag{36}$$

$$U(n) = \{U_b'[q_b^+(n)] - SU_b'[q_b^-(n)]\}H(n - z/m) + \{SU_a'[q_a^-(n)] - U_a'[q_a^+(n)]\}H(n - z), \tag{37}$$

$$W(n) = \{W_b'[q_b^+(n)] + W_b'[q_b^-(n)]\}H(n - z/m) - \{W_a'[q_a^+(n)] + W_a'[q_a^-(n)]\}H(n - z), \tag{38}$$

where the primed functions of q follow from (21), (27) and (30) upon multiplication by q. Again, the transformations (31) may prove useful in evaluating the integrals.

6. Rayleigh pole effects. When $z/r \to 0$ care must be taken in evaluating (25), (28), (35) and (36) because the hyperbolic Cagniard contours collapse onto the positive Im(q)-axis. This necessitates deforming the contours about the Rayleigh pole due to the presence of D in the integrand denominators, which results in special contributions to the solution. In this section we isolate these Rayleigh pole contributions for all $r, z, s > 0$ by following the approach of [3]. The contributions are then briefly studied for the case $z = 0$. The inverse Laplace transform [14] is defined as

$$F(s) = \frac{1}{2\pi i}\int_{p_0 - i\infty}^{p_0 + i\infty} \hat{F} e^{ps}\, dp, \tag{39}$$

where the positive real constant p_0 is large enough to insure convergence of (6a) and that the integration path lies to the right of all singularities of $\hat{F}$. Operating on (14) with (39) therefore yields

$$\mu u = \frac{1}{2\pi i}\int_0^s f h \int_0^\infty J_1(\xi r) J_1(\xi h) \int_{\varepsilon - i\infty}^{\varepsilon + i\infty} [2\alpha\beta e^{-\beta z} - (\beta^2 + \xi^2) e^{-\alpha z}] \frac{e^{p(s-t)}}{R}\, dp\, d\xi\, dt, \tag{40}$$

where $\varepsilon \to 0$. Because the p-integrand is analytic for Re(p) > 0, the p-integral can be evaluated by switching the integration path into the left half of the p-plane. To insure that the integrand is bounded there for $|p| \to \infty$ we must have $t < s$. The Rayleigh function R has zeros at $p = \pm i m_R \xi$, which, because ξ is real and positive, lie on the Im(p)-axis in (40). Thus, in switching integration paths by means of the Cauchy theorem, both poles will be crossed and their residues will appear in the solution as the Rayleigh pole contribution. Denoting this contribution by u_R, we find

$$\mu u_R = \frac{m^2}{2m_R G}\int_0^s f h \,\mathrm{Im} \int_0^\infty J_1(\xi r) J_1(\xi h)[2cd e^{i\xi Q} - (1 + d^2) e^{i\xi P}]\, d\xi\, dt, \tag{41}$$

$$P = m_R(s - t) + icz, \qquad Q = m_R(s - t) + idz, \tag{42}$$

$$c = \sqrt{(1 - m_R^2)}, \qquad d = \sqrt{(1 - m_R^2/m^2)}, \qquad G = \frac{1}{cd}[c^2 + m^2 d^2 - cd(1 + d^2)]. \tag{43}$$

In view of (17),

$$\int_0^\infty J_1(\xi r) J_1(\xi h) e^{i\xi P}\, d\xi = \frac{4}{rh\pi^2}\int_0^h \int_0^r \frac{xy}{XY}\int_0^\infty \sin \xi x \sin \xi y e^{i\xi P}\, d\xi\, dy\, dx. \tag{44}$$

Because $z > 0$ it is readily shown that, after some rearranging of terms,

$$\int_0^\infty \sin \xi x \sin \xi y e^{i\xi P}\, d\xi = \frac{1}{2i}\left[\frac{(P - x)^2}{(P - x)^2 - y^2} - \frac{(P + x)^2}{(P + x)^2 - y^2}\right]. \tag{45}$$

Substitution of (45) and formally carrying out the indicated y-integration gives for the right-hand side of (44)

$$\frac{1}{\pi rh}\int_0^h \frac{x}{X}\left[\frac{P - x}{\sqrt{[r^2 - (P - x)^2]}} - \frac{P + x}{\sqrt{[r^2 - (P + x)^2]}}\right] dx = \frac{1}{rh} I_u(P), \tag{46}$$

which can be simplified to yield

$$I_u(P) = \pm\frac{2}{\pi}\int_{-h}^h \frac{x(P \pm x)\, dx}{X\sqrt{[r^2 - (P \pm x)^2]}}, \qquad \pm\frac{2}{\pi}\int_{-r}^r \frac{y(P \pm y)\, dy}{Y\sqrt{[h^2 - (P \pm y)^2]}}. \tag{47}$$

Thus, (41) can be rewritten as

$$\mu r u_R = \frac{m^2}{2m_R G} \int_0^s f[2cd \text{ Im } I_u(Q) - (1 + d^2)\text{Im } I_u(P)]\, dt. \tag{48}$$

Similarly, the total Rayleigh pole contribution to w can be written as

$$\mu w_R = \frac{m^2 c}{2m_R G} \int_0^s f[2 \text{ Im } I_w(Q) - (1 + d^2)\text{Im } I_w(P)]\, dt, \tag{49}$$

$$I_w(P) = 1 - \frac{2i}{\pi} \int_{-r}^{r} \frac{(P \pm y)\, dy}{Y\sqrt{[h^2 - (P \pm y)^2]}}, \qquad \pm \frac{2i}{\pi} \int_{-h}^{h} \frac{x\, dx}{X\sqrt{[r^2 - (P \pm x)^2]}}. \tag{50}$$

Turning to the spatially-varying problem in Sec. 5, we find that

$$\mu r u_R = \frac{m^2}{2m_R^2 G} \int_0^s h\dot{h} g(h)[(1 + d^2)\text{Re } I_u(P) - 2cd \text{ Re } I_u(Q)]\, dt, \tag{51}$$

$$\mu w_R = \frac{m^2 c}{2m_R^2 G} \int_0^s h\dot{h} g(h)[(1 + d^2)\text{Re } I_w(P) - 2 \text{ Re } I_w(Q)]\, dt, \tag{52}$$

where in this case $I_u(\ )$ follows from (50) by interchanging h and r while

$$I_w(P) = -\frac{2}{\pi} \int_{-h}^{h} \frac{dx}{X\sqrt{[r^2 - (P \pm x)^2]}}, \qquad -\frac{2}{\pi} \int_{-r}^{r} \frac{dy}{Y\sqrt{[h^2 - (P \pm y)^2]}}. \tag{53}$$

As indicated above, the Rayleigh pole contribution to the solution is most noticeable on the half-space surface ($z = 0$). Therefore, we study these contributions for the normal displacements. When $z = 0$ we have $P, Q = m_R(s - t)$ so that Eqs. (49) and (52) can be simplified to yield, respectively,

$$\mu w_R = -\frac{2m_R c}{\pi G} \int_0^s \frac{f}{x_1} [x_3 \Pi(x_4, x_2) + x_5 K(x_2)]\, dt, \tag{54}$$

$$\mu w_R = \frac{2c}{\pi G} \int_0^s h\dot{h} g(h) \frac{1}{x_1} K(x_2)\, dt, \tag{55}$$

where K and Π are the complete elliptic integrals of, respectively, the first and third kinds of parameter x_4 and modulus x_2 [17]. The quantities x_1, x_2, x_3, x_4 and x_5 in (54) and (55) are defined in the Appendix. It should be noted, however, that the simple forms of (54) and (55) are not necessarily the most convenient for computational purposes. In view of the Appendix it can be shown that as $|r - h| \to m_R(s - t)$

$$\frac{2}{x_1}(x_3 \Pi + x_5 K), \quad \frac{2hK}{x_1} \simeq \sqrt{\left(\frac{h}{r}\right)} \ln | \, |r - h| - m_R(s - t)| + \cdots, \tag{56}$$

while for $r + h = m_R(s - t)$

$$\frac{2}{x_1}(x_3 \Pi + x_5 K), \quad \frac{2hK}{x_1} = \frac{\pi}{2} \sqrt{\left(\frac{h}{r}\right)}. \tag{57}$$

Eqs. (54)–(57) demonstrate that the pressure zone edge in general creates logarithmic singularities in $\dot{w}$ which travel both radially inward and outward at the Rayleigh wave speed. However, (57) shows that when the inwardly-traveling wave crosses the pressure

zone center, the singularity disappears. Moreover the singularity in general decays as $0(r^{-1/2})$, $r \to \infty$. This attenuation is identical to that observed in [3] for the point force.

To gain insight into the effect of zone time-history on the solution behavior, the Rayleigh pole contribution (54) due to four different functions h is studied. The surface point $z = 0, r = 1.0$ is examined for a time interval $s \geq 1/m_R$ under a constant pressure p_0, where "1.0" is some unit of length. The h-functions are

$$h(s) = 0.5m_R s, \qquad h(s) = 1.5m_R s, \qquad h(s) = 1.0 + \cos \pi s, \qquad h(s) = 0.5s^2 \quad (58a\text{–}d)$$

and m takes the typical value $1/\sqrt{3}$. Because w_R, r, s and h have the same dimension, (54) and (58) show that the choice of unit length can be arbitrary, and that these quantities will be multiples of this length. Eqs. (58a–d) represent pressure zones with, respectively, constant sub- and supercritical, oscillatory and constantly increasing extension rates.

Plots of (54) are shown in Fig. 3. The singular behavior in the particle velocity predicted by (56) is evident as $s \to 1/m_R$. The magnitude of all the Rayleigh disturbances tend to increase with s and the type of increase appears to be related to the time-history of the h-functions. Thus, the magnitude due to the zone with the constant supercritical extension rate exceeds that due to the constant subcritical rate. Moreover, the sinusoidally oscillating zone produces an oscillation in the time behavior of the corresponding magnitude. The constantly-increasing zone velocity gives, after a short interval, a magnitude whose slope also increases while the slopes due to the constant-velocity zones become constant. From the discussion of [18], it is noted that, if the Rayleigh wave itself is of interest, values of s in Fig. 3 should be confined near $1/m_R$.

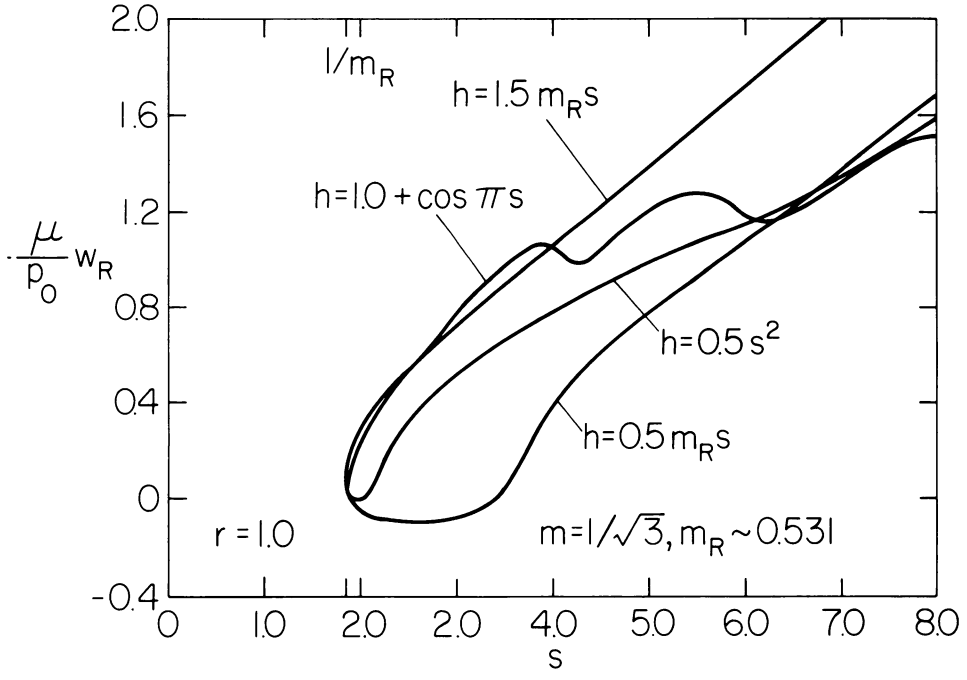

FIG. 3. Rayleigh pole disturbances for different pressure zones under constant pressure.

7. Other wave propagation aspects. For more insight into the solution behavior, apart from the Rayleigh pole contributions, it is convenient, in light of (22) and (23), to write the U_a and U_b terms from (26) in the more explicit forms

$$U_a[q_a^{\pm}(s-t)]H(s-t-\rho_{\pm}) + U_a[iv_a^{\pm}(s-t)]H(\rho_{\pm}+t-s)H(s-t-z), \tag{59}$$

$$U_b[q_b^{\pm}(s-t)]H[m(s-t)-\rho_{\pm}] + U_b[iv_b^{\pm}(s-t)]H[\rho_{\pm}-m(s-t)]H[m(s-t)-z]. \tag{60}$$

At some instant t, suppose a point on the pressure zone edge in a given axial plane is located at $r = h(t)$. For $s \geq t$ this edge point and its diametrical opposite, or image point, will radiate dilatational and rotational signals behind circular wave fronts in the axial plane whose radii are, respectively, $s - t$ and $m(s-t)$. At t the distance from the edge point and its image to a point r, z in the same axial plane are $\sqrt{(z^2 + |r-h|^2)}$ and $\sqrt{[z^2 + (r+h)^2]}$, respectively. In view of this illustration and the Heaviside functions, the first terms in (59) and (60), i.e. along the hyperbolic Cagniard contours, represent, respectively, dilatational and rotational disturbances generated by a point on the pressure zone edge $(-)$ and its mirror image $(+)$.

Examination of (21), (22) and (27) shows that if $z \geq r_{\pm}\sqrt{(m^{-2}-1)}$, then for all $z \leq s-t$, $m(s-t) \leq \rho^{\pm}$ we have $0 \leq v_a^{\pm}, v_b^{\pm} \leq 1$ so that the second terms in (59) and (60) are purely real. However, if $z \leq r_{\pm}\sqrt{(m^{-2}-1)}$, while $v_a^{\pm} \leq 1$ still, we now have $1 \leq v_b^{\pm} \leq 1/m$ for $r_{\pm} + z\sqrt{(m^{-2}-1)} \leq m(s-t) \leq \rho_{\pm}$ and the second term in (60) is complex. Returning to the previous illustration, it can be seen that the relations $z \leq |r \pm h|\sqrt{(m^{-2}-1)}$, $|r \pm h| + z\sqrt{(m^{-2}-1)} \leq \sqrt{[z^2 + (r \pm h)^2]}$ confine r, z within regions bounded by the edge and image point circles of radius $m(s-t)$ and tangents to these circles which intersect the circles of radius $s - t$ at the half-space surface. In this light, the complex contribution above represents the head wave disturbances, i.e., rotational waves generated by the faster-traveling dilatational waves radiating from the edge $(-)$ and image $(+)$ points.

Moreover, if we visualize that, in the same illustration, the zone edge moves a finite distance instantaneously at t, then instead of points, an edge strip and its image result. Between the ends of the strip, the envelopes of the circular wavefronts radiated by points in the strip are straight lines parallel to the half-space surface and a distance $m(s-t)$ or $s - t$ from it if the radiated signals are, respectively, dilatational or rotational. In view of the Heaviside function products, it follows that real values of the second terms in (59) and (60) are related to the plane dilatational and rotational waves generated when the pressure zone radius $h(s)$ changes instantaneously.

An instantaneous change in h is a limit case of a supersonic zone velocity, i.e., $|\dot{h}| \to \infty$. In our now well-worn illustration, it is clear that for finite $\dot{h}$ points r, z behind the circle of radius $m(s-t)$ radiating from the zone edge point are confined within a locus $C_-(t) = m^2(s-t)^2 - z^2 - |r-h|^2$. Solution of the characteristic equations

$$C_- = 0, \qquad dC_-/dt = 0 \tag{61}$$

gives an envelope for varying t of the form

$$r = \frac{m^2}{\dot{h}}(s-t) + h, \qquad z = m(s-t)\sqrt{\left(1 - \frac{m^2}{\dot{h}^2}\right)} \tag{62}$$

which obviously yields real values only for $\dot{h} > m$. In view of the Heaviside functions in (60), this result shows that if $\dot{h}(s) > m$ for $s \geq s_0$, then a rotational Mach wave front

defined by (62) arises, where $t = s_0$. This wavefront emanates from the pressure zone edge $z = 0$, $r = h(s)$ and is tangent to the circle $C_-(s_0) = 0$. If subsequently at $s_1 > s_0$ $\dot{h}(s)$ drops below m, then the wavefront separates from the edge and also becomes tangent to the circle $C_-(s_1) = 0$. Eq. (62) describes a straight line when $\dot{h} = \text{constant} > m$. This equation is also valid for $\dot{h} < 0$, $|\dot{h}| > m$ when $r > 0$. Therefore, an inwardly-traveling Mach wave will result from zone contraction rates which exceed the rotational wave speed.

A similar analysis for the image locus $C_+(t) = m^2(s-t)^2 - z^2 - (r+h)^2$ gives

$$r = -\frac{m^2}{\dot{h}}(s-t) - h, \qquad z = m(s-t)\sqrt{\left(1 - \frac{m^2}{\dot{h}^2}\right)} \tag{63}$$

where the necessary combination $\dot{h} < 0$, $|\dot{h}| > m$, $r > 0$ is possible. The pressure zone is not allowed to contract to a point so that the edge passes through itself. However, (63) can describe a wavefront traveling through the zone center which previously had separated from the zone edge when the contraction rate dropped below the rotational wave speed. It should be noted that a similar discussion applies for dilatational Mach waves by setting $m = 1$.

8. Brief summary. Two problems of pressure distributions applied to a half-space axisymmetrically over a circular pressure zone whose radius changes at a non-uniform rate have been considered. General solutions for the displacements in both problems were obtained by transform techniques. A brief investigation of these expressions showed that the wave propagation disturbances are generated at the pressure zone edge. The form of the displacements indicated that the disturbance arising at a location in the half-space in general depends on the signals received both from a point on the zone edge having the same polar angle and the diametric opposite, or image, edge point.

More particularly, it was found that Mach waves can be generated which travel radially outward or inward, depending on whether the zone edge is expanding or contracting at a rate which exceeds the dilatational and/or rotational wave speeds in the half-space. A general formulation for the contributions due to the Rayleigh pole existing in the transform solutions showed that, on the half-space surface, logarithmic singularities in the normal particle velocity travel both radially inward and outward from the pressure zone edge with the Rayleigh wave speed. These singularities decay with the square-root of the radius from the pressure zone center and disappear at the center.

A complete study of the solutions for different zone time-histories was beyond the scope of the present general work. However, the Rayleigh pole disturbances on the half-plane surface for a uniform pressure applied over zones with different time-histories were examined. The results indicated that some characteristics of the type of history may be manifested in the time-history of the corresponding Rayleigh disturbance. Perhaps, then, information on the time variation of a pressure zone can be obtained from studies of the Rayleigh wave itself. It should be noted, however, that such studies must also include the effect of the pressure distribution over the zone. A survey of [4–11] may give insight into this effect. More work on both effects is currently planned.

It should be noted that two closely related problems not treated here are analogous to the two-dimensional moving line load problem of [13], i.e. the expanding ring load

problems. These problems can be formulated by substituting for σ_z in (1a) and (32), respectively, the expressions

$$\sigma_z = -f(s)\,\delta[h(s) - r], \qquad \sigma_z = g(r)\,\delta(h_0 - r) - g(r)\,\delta[h(s) - r] \tag{64a,b}$$

when $z = 0$. These problems are readily solvable by the methods outlined here. Moreover, it is clear that the solutions for (64a) are, in form, the negative of the derivatives with respect to r of the present time-dependent problem. For (64b) the solutions follow by adding the results for the present spatially-varying problem with g replaced by $g_{,r}$ to the negative of the derivative of the results themselves.

Appendix. In (54)–(57) we define

$$x_\pm = \pm r - m_R(s - t) \tag{A.1}$$

so that for $x_- < -h < x_+ < h$:

$$x_1 = 2\sqrt{(rh)}; \qquad x_1 x_2 = \sqrt{(h + x_+)}\sqrt{(h - x_-)}; \qquad x_3 = h + x_-, x_+ - h \tag{A.2}$$

$$2rx_4, 2hx_4 = h + x_+; \qquad x_5 = x_-, h \tag{A.3}$$

while for $x_- < -h < h < x_+$:

$$x_1 = \sqrt{(h + x_+)}\sqrt{(h - x_-)}; \qquad x_1 x_2 = 2\sqrt{(rh)}; \qquad x_3 = h + x_-, h - x_+ \tag{A.4}$$

$$(h - x_-)x_4, (h + x_+)x_4 = 2h; \qquad x_5 = x_-, x_+ \tag{A.5}$$

while for $-h < x_- < h < x_+$:

$$x_1 = 2\sqrt{(rh)}; \qquad x_1 x_2 = \sqrt{(h + x_+)}\sqrt{(h - x_-)}; \qquad x_3 = h + x_-, h - x_+ \tag{A.6}$$

$$2hx_4, 2rx_4 = h - x_-; \qquad x_5 = -h, x_+ \tag{A.7}$$

and for $-h < x_- < x_+ < h$:

$$x_1 = \sqrt{(h + x_+)}\sqrt{(h - x_-)}; \qquad x_1 x_2 = 2\sqrt{(rh)}; \qquad x_3 = h + x_-, x_+ - h \tag{A.8}$$

$$(h + x_+)x_4, (h - x_-)x_4 = 2r; \qquad x_5 = -h, h. \tag{A.9}$$

It is understood that in any of the four possible sets of x_3, x_4 and x_5, the parameters chosen must *all* be either left- or right-hand entries.

References

[1] H. Lamb, Phil. Trans. Roy. Soc. (London) **A203**, 1 (1904)
[2] C. L. Pekeris, Proc. Nat. Acad. Sci. (USA) **41**, 469 (1955)
[3] C. C. Chao, H. H. Bleich, and J. Sackman, J. Appl. Mech. **28**, 300 (1961)
[4] J. W. Craggs, Proc. Camb. Phil. Soc. **59**, 803 (1963)
[5] C. Atkinson, Int. J. Engng. Sci. **6**, 27 (1968)
[6] D. C. Gakenheimer, J. Appl. Mech. **38**, 99 (1971)
[7] J. W. Miles, J. Appl. Mech. **27**, 710 (1960)
[8] M. L. Baron and R. Check, J. EMD, Proc. ASCE, **87**, 33 (1961)
[9] C. M. Ablow, in *Proc. 4th U.S. Natl. Cong. Appl. Mech.*, 51 (1962)
[10] R. M. Blowers, J. Inst. Math. Appl., **5**, 167 (1969)
[11] K. J. Tong, *Dynamic response of a homogeneous isotropic elastic half-space to a spreading blast wave*, Ph.D. Thesis, Stanford Univ., Stanford, California, Dec. 1968

[12] L. B. Freund, Quart. Appl. Math. **30**, 271 (1972)
[13] L. B. Freund, J. Appl. Mech. **40**, 699 (1973)
[14] I. N. Sneddon, *The use of integral transforms*, McGraw-Hill, New York, 1972, Chs. 3, 5, 9
[15] A. T. de Hoop, Appl. Sci. Res. **B8**, 349 (1960)
[16] G. N. Watson, *A treatise on the theory of Bessel functions*, Cambridge University Press, 1966, 170
[17] I. S. Gradshteyn and I. M. Ryzhik, *Table of integrals, series and products*, Academic Press, New York, 1965, 241
[18] J. D. Achenbach, *Wave propagation in elastic solids*, North-Holland, Amsterdam, 1973, 320